Snap-through of elastic bistable beam under contactless magnetic actuation

A. Amor, Amâncio Fernandes, J. Pouget

Snap-through of elastic bistable beam under contactless magnetic actuation

A. Amor[a], A. Fernandes[a,*], and J. Pouget[a]

[a]Sorbonne Université, CNRS, Institut Jean le Rond d'Alembert, UMR 7190, F-75005 Paris, France;
[*]Corresponding author, amancio.fernandes@sorbonne-universite.fr

November 25, 2020

Abstract

We propose the modeling of contactless switching of a bistable slender beam using Laplace force actuation. The model beam is based on the elastica approach which allows large amplitudes of the cross-section rotation and large elastic transformations. Furthermore, the extensibility of the elastic beam is accounted for and it plays a crucial role in the switching process. The study is devoted particularly to the actuation mechanism of the bistable beam uniformly loaded by a density of lineic force which is permanently perpendicular to the beam deformation. Such actuation can be produced by the Laplace force due to an electric current travelling along the beam placed in a magnetic induction. The mechanism of the bistable switching is analyzed in detail using a variational formulation and stable and unstable equilibria are described. We investigate numerically the post-buckling behavior to capture the exact buckling modes that follow the path in the unstable region. The numerical simulations are also used to obtain the bistable response in terms of actuating force (or electric current amplitude), beam end-shortening and mid-point displacement of the beam. We also perform a finite element computation and provide a validation of the results obtained by solving the set of equations of the boundary value problem.

The second part of the work is focussed on the experimental validation of the switching mechanism of the bistable beam presented in the analytical part. We design an experimental set-up for the fine measurement of the mid-point displacement of the bistable beam as a function of the electric current travelling the beam. The region of bistable instability is revealed by experimental adjustment of the bifurcation point associated with the actuating force. All the results extracted from experimental tests are compared to those coming from the modeling investigations, which ascertains with good accuracy the approach of the proposed model for bistable beam.

Keywords : Bistable mechanism; buckling; snap-through; Laplace force; bifurcation.

1 Introduction

Consider an elastic slender beam. One end of the beam is fixed, the other one undergoes a small end-shortening caused by a compressive force applied in the direction of the beam axis. As long as the force is weak, less than a certain critical value, the beam is in compression as predicted by linear elasticity. As soon as the force exceeds a critical value, the beam is no longer straight, and undergoes a transverse deformation or deflection (Bazant, Cedolin , 1991; Bigoni , 2012; Dym , 2002; Thomson and Hunt , 1973). The amplitude of deflection increases with end-shortening as well

as with compressive force. We are faced with a bifurcation phenomenon, resulting in the buckling of the beam (Timoshenko and Gere , 1963). The later can deflect either upwards or downwards. The elastic structure that we are describing is a bistable system and both positions of the beam (upwards or downwards) are stable states. However, the most interesting aspect of this bistable system is to be able to switch from one stable state to another regardless of how the transition is completed. Although a great emphasis has been paid to beam buckling and several studies are available in the literature, the mechanism of switching between stable positions remains an active topic of research, especially because a linear model is inadequate and recourse to a nonlinear model becomes inescapable. Furthermore, some questions are raised such as how does the bistable system switch between stable positions and what are the buckling modes which are involved in the process?

Actuating a bistable beam to force it to switch can be accomplished using various means. A first idea is to load laterally the beam with a punctual force at any point of the beam, or with a punctual moment applied to the beam in the direction perpendicular to plane deformation (Cleary and Su , 2015). However, the bistable beam response under an applied punctual force depends on the way of applying the force, more precisely, on whether the force is vertically fixed onto the midpoint of the elastic beam or if the force stays on a central line between beam ends while the bistable snaps. Loading a bistable beam with a vertical force which is always fixed onto the beam has been reported in some studies, among them Pippard (Pippard , 1990) and Patricio (Patricio *et al.* , 1998). Nevertheless, this situation is not convenient for experimental considerations. An extensive study of the actuation of a bistable beam by punctual force along a fixed central line in space (not necessarily on the midline) has been presented in (Camescasse *et al.* , 2013) and experimental validation of the model has been discussed in (Camescasse *et al.* , 2014). A comparative study has been proposed by (Chen and Hung , 2011) according to the way of applying the force onto the beam force while the latter is switched. Then Cheng and Hung examine three cases : (i) the force is attached onto the beam mid-point, (ii) the force is applied along a fixed central line in space and (iii) the force is applied by means of a device such that the force is always perpendicular to the deformed beam and its point of application is allowed to slide on the beam, while staying along the central line in space.

Switching or snapping-through of bistable systems can be obtained by means of active materials such as piezoelectric ceramics, shape memory alloys, electroactive polymers or magnetostrictive materials to cite the most popular. In this situation, the active elements bonded onto the elastic beam are able to induce local strains or stresses onto the buckled beam to control the switching process (Maurini *et al.* , 2007).

In each the above-mentioned situations, the actuation is in contact with the bistable system and the influence of the actuating mechanism must be accounted for. The present study proposes an innovative means of actuating a bistable system by a uniform density of lineic force, which is able to trigger the snap-through of the buckled beam as soon as the density of force is great enough to make the bistable pass through the zone of instability to reach the other stable position. Here, the loading mechanism is such that the lineic density of force is permanently fixed onto the beam. Moreover, when the beam is deformed while switching, the lineic force stays perpendicular to the beam deformation. Such a loading mechanism can be properly produced by the Laplace force (Griffiths , 1999; Jackson , 1998). More precisely, this is the force applied to an electrically conductive wire traversed by a volume density of electric current placed in a magnetic induction field. The elementary force is then perpendicular to the plane formed by the magnetic induction vector and vector of the electric current density or, in other words, the tangent vector to the deformed

beam.

One of the main purposes of the present study is to investigate the bistable buckled beam on the basis of the elastica model, especially because a rather small disturbance of the actuating work can produce displacement and cross-section rotation of the beam of relatively large amplitudes. Bistable buckled beam modeling is subject of numerous research studies which can be divided in different approaches according to the starting hypothesis. Elastica model has been extended to elastic arches loaded at its center by Pippard (Pippard , 1990). Vangbo (Vangbo , 1998) investigated the switching response of a bistable beam including the compressive effect by using an expansion of the solution to the beam equation on the buckling modes. In the framework of modal formulation, the detailed behavior of the stable and unstable branches of the bistability response under loading has been proposed by (Cazottes *et al.* , 2010). These authors have examined on the basis of a similar modeling, that is, buckling modal formulation, the actuation of a bistable buckled beam subject to a moment (Cazottes *et al.* , 2008). Beside the elastica beam theory, some weakly nonlinear approches are often considered. In particular, a theory accounting for extensibility of the beam leads to geometric nonlinearity combining bending and stretching deformations. This kind of approach has been developed by Nayfeh and Enam (Nayfeh and Enam , 2008) for a buckled beam and by Pinto and Gonçalves (Pinto and Gonçalves , 2002) for a simply supported shallow elastic arch. The weakly nonlinear approach has been considered also for both static and dynamic snap-through of bistable structures by Chandra *et al.* (Chandra *et al.* , 2013). The present work is devoted to the bistable beam but we also mention some extensions of bistability effect and even tristability to elastic thin plates or shells. Such studies have been conducted by Schultz *et al.* (Schultz *et al.* , 2006) for bistability control of composite plates using piezoelectric actuators, or by Vidoli and Maurini (Vidoli and Maurini , 2008) for tristability of thin orthotropic shells, or by Fernandes *et al.* (Fernandes *et al* , 2010) for the study of shape control of bistable composite plates.

One of the most attractive development of bistable systems (or multistable systems by extension) is their ability to be miniaturized from millimeter scale to dimensions of the order of the micron. Such bistable systems become particularly interesting to design microelectromechanical devices (MEMS). At the microscopic scale, the actuation making use of Lorentz force is quite attractive. According to the Lorentz theory of electrons, the force on an electric punctual charge consists of two parts. The first part is a force produced by an electric field on an electric charge (electrostatic force). The second part is the force applied to a moving electric charge placed in a magnetic induction. When the material deals with a continuum of density (per unit of volume or mass) of electric charge, the Lorentz force becomes a kind of effective Lorentz force. Subsequent use of Lorentz force leads to the notion of a so-called ponderomotive force or electromagnetic force. More precisely, the latter force is deduced by applying the classical Lorentzian (space) averaging procedure to an assembly of electric punctual charge contained within a microelement of volume ΔV (Maugin , 1988). The macroscopic quantities thus obtained by this spatial averaging procedure are considered to be sufficiently smooth functions of space and time. Now, going back to our problem, if the charges are travelling in a conductive wire placed in a magnetic induction, the force acting on the wire is called the Laplace force (Griffiths , 1999; Jackson , 1998). Obviously, we then have a contactless actuation of the bistable system. Moreover, such electromagnetic actuations are easily controlled using electronic circuits.

Electromechanical system technology presents important advantages including, small size, light weight, limited energy consumption and integrated electronic components. Electrostatic force has been exploited to excite sensors at their resonant frequencies, based on bistable concept (Herrera-

May *et al.* , 2009). The actuation of a micro-arch subject to electrostatic force due to a difference of electric potential between a semi-infinite rigid electrode and the initially curved beam has been analyzed for applications to MEMS (Das and Batra , 2009; Pane and Asano , 2008; Williams *et al.* , 2012). Park and Hah (Park and Hah , 2008) present a study of the actuation of pre-shaped beam controlled by electromagnetic force and experimental validation of the snap-through mechanism of the bistable micro-beam is also conducted. Some other interesting works concerning micro-systems based on bistable beam have been conducted mainly by Buchaillot *et al.* (Buchaillot *et al.* , 2008), Krylov and Dick (Krylov and Dick , 2010) or Krylov *et al.* (Krylov *et al.* , 2011).

Actuating a bistable beam by means of active materials is an interesting development in order to control the stability of the bistable beam during the snap-through process by using electric field, gradient of temperature or magnetic induction. Such materials induce local strains leading to trigger switching the bistable beam as soon as the strain is large enough to enter the unstable zone. Electrostatically actuated bistable systems are well adapted for controlling the bistability and they are perfectly designed for MEMS (Krylov *et al.* , 2011; Medina *et al.* , 2018). Deformation of a bistable beam bonded with a piezoelectric element is induced by elongation or compression in the piezoelectric layer by means of the application of an appropriate electric field. Aimmanee and Tichakorn (Aimmanee and Tichakorn , 2018) have proposed such an actuation of a bistable beam using smart materials. A study of distributed multiparameter actuation for the buckling and snap-through control of a pinned elastic beam was reported in (Maurini *et al.* , 2007). There, the authors propose an elastic beam sandwiched by two pairs of piezoelectric actuators driven by two differences of electric potential. An extension to the bistable shell made of magnetic rubber composite using the magnetic actuation of the shell cap has been conducted by (Seffen and Vidoli , 2016).

The present work is based on an extensible elastica beam model. We describe the beam deformation by two strain measures which are the extension strain along the beam axis and the beam curvature. The beam kinematic is presented in the next section (Section 2). Both descriptions in the fixed frame and local frame attached to the beam deformation are given in that section. We then derive the equations of the buckled beam from the virtual work principle. Section 3 is devoted to this task. Moreover, the boundary conditions - clamped-clamped beam - are specified in the same section. Section 4 deals with the numerical study of the set of nonlinear boundary value problems. The numerical problem thus stated relies on the model equations based on the shooting method associated with a numerical procedure to capture the unknown shooting parameters. In the same section we compare the solutions derived from the model equations to those obtained with the help of the finite element method. One of the main results coming from the numerical investigations is the bistable response, that is, the actuating driving force (or the electric current) as a function of the beam mid-point displacement. The results are discussed according to the chosen parameters (geometry of the beam, the end-shortening). A part of the work is devoted to the experimental validation of the proposed model (Section 5). We report the investigation of the experimental measurements in Section 5 and discuss the results thus obtained and compare them to those deduced from the model and numerical simulations.

2 Description of the bistable system

2.1 Kinematics

We consider an elastic beam clamped at each of its ends and having length L_0 at rest. The left end is fixed while the right end is subject to an end-shortening of small amount ΔL. The cross-section of the beam is homogeneous and rectangular with a width b and thickness h. A fixed Cartesian reference frame $\{A; \mathbf{e_1}, \mathbf{e_2}, \mathbf{e_3}\}$ is attached to the structure in its initial configuration $\mathcal{R}_0$. The reference frame is such that the unit vector $\mathbf{e_1}$ lies in the direction of the beam axis. Due to the end-shortening, the distance between clamps becomes $L = L_0 - \Delta L$. The elastic beam is initially straight and free of stress (see Fig.1.a for a sketch). The beam undergoes a buckling caused by the imposed end-shortening at the right end which is the current configuration. A compressive force P is associated to the end-shortening and it can be viewed as the conjugate variable of the end-shortening ΔL. This force will be determined once the problem is completely solved. The beam in the reference configuration is described by the set

$$\mathcal{R}_0 = \{\mathbf{OG_0} = \mathbf{q_0}(s) = s\ \mathbf{e_1}, \quad \text{with} \quad s \in [0, L_0]\} \tag{1}$$

where s is the abscissa along the beam axis and $\mathbf{q_0}(s)$ is the position vector of the material point G_0. The deformed beam in the current configuration is a smooth curve (see Fig.1.b). The point G_0 in the initial configuration is then transformed into the material point G of the deformed beam given by

$$\mathbf{OG} = \mathbf{q}(s) = x(s)\ \mathbf{e_1} + y(s)\ \mathbf{e_2}, \qquad s \in [0, L_0]\ . \tag{2}$$
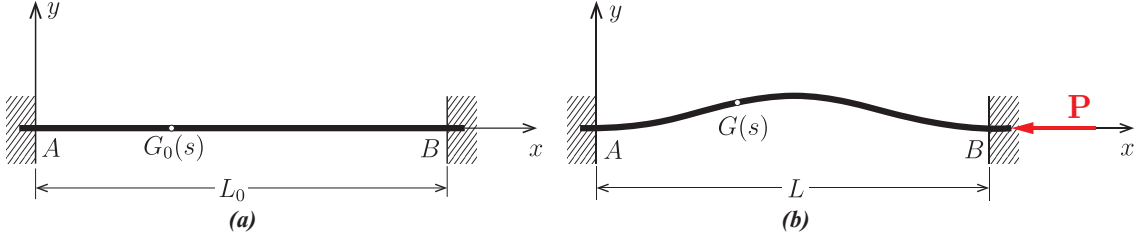

Figure 1: Clamped-clamped elastic beam: (a) Beam in the reference configuration at rest (no load) (b) Beam in its buckled configuration.

We denote by $\boldsymbol{\tau}$ the unit vector tangent to the curve describing the deformed beam at the point $G(s)$. The tangent vector is defined by

$$\boldsymbol{\tau} = \frac{d\mathbf{q}}{d\bar{s}}, \tag{3}$$

where $\bar{s}$ is the curvilinear coordinate measured along the deformed beam. In addition, we introduce $\Lambda = \frac{d\bar{s}}{ds}$, the ratio of the length of differential line element of the beam in the deformed configuration to that of the undeformed configuration. The parameter Λ measures the extensibility of the beam. The normal unit vector $\mathbf{n}$ is perpendicular to the tangent vector $\boldsymbol{\tau}$. Accordingly, the set of orthogonal unit vectors $\{\boldsymbol{\tau}, \mathbf{n}, \mathbf{e_3}\}$ forms the local frame attached to the deformed beam at the curvilinear abscissa $\bar{s}$. These vectors can be written in the reference frame $\{A; \mathbf{e_1}, \mathbf{e_2}, \mathbf{e_3}\}$ using the following

transformation

$$\boldsymbol{\tau}(s) = \quad \cos\theta(s)\ \mathbf{e_1} + \sin\theta(s)\ \mathbf{e_2}\,, \tag{4a}$$

$$\mathbf{n}(s) = -\sin\theta(s)\ \mathbf{e_1} + \cos\theta(s)\ \mathbf{e_2}\,, \tag{4b}$$

where the angle of rotation θ is $\theta = \widehat{(\mathbf{e_1},\boldsymbol{\tau})}$.
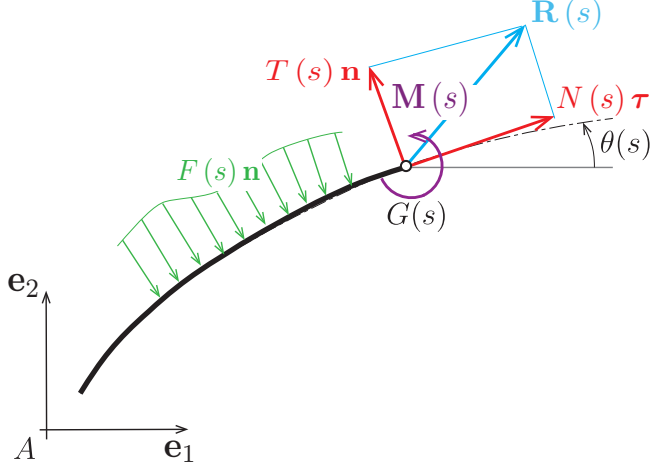

Figure 2: A part of the beam in the deformed configuration: (i) Internal actions (force and moment) at the material point $G(s)$, (ii) Fixed and local frames.

The reader is referred to Fig.2 for the sketch of different vectorial variables used in the forthcoming sections. The gradient of the beam transformation characterized by the vector $\mathbf{q}(s)$ can be easily obtained from Eqn. (3) accounting for the extensibility Λ of the beam and it can be written down as

$$\mathbf{q}' = \Lambda\boldsymbol{\tau}\,, \tag{5}$$

where the prime is the derivative with respect to the curvilinear abscissa s.

The extensional strain ε and the beam curvature κ are chosen as the two strain measures. They are given by

$$\varepsilon = \Lambda - 1\,, \tag{6}$$

$$\kappa = \theta_{,\bar{s}} = \frac{d\boldsymbol{\tau}}{d\bar{s}}\cdot\mathbf{n} = \frac{1}{\Lambda}\theta_{,s}\,. \tag{7}$$

The vector position in the current configuration of the beam is written in the local frame $\{G;\boldsymbol{\tau},\mathbf{n},\mathbf{e_3}\}$ given by

$$\mathbf{q}(s) = q_T(s)\ \boldsymbol{\tau} + q_N(s)\ \mathbf{n}\,, \tag{8}$$

which can be compared to that of given by Eqn. (2). Consequently, we have the choice to compute the beam transformation either in the reference frame $\{A;\mathbf{e_1},\mathbf{e_2},\mathbf{e_3}\}$ or in the local frame $\{G;\boldsymbol{\tau},\mathbf{n},\mathbf{e_3}\}$ by sake of convenience. The formulation from one frame to the other can be obtained by using Eqn. (4). The geometric relations Eqn. (5) become

$$q_T' - \theta' q_N = \Lambda\,, \tag{9a}$$

$$q_N' + \theta' q_T = 0\,. \tag{9b}$$

In the forthcoming sections, especially for the variational formulation, the use of variables defined in the local frame will be most useful.

2.2 Constitutive equations of the beam

The beam cross-section is rectangular and homogeneous and it undergoes internal resultants in force and moment which is defined as distributor of the internal actions given by the set $\{\mathbf{R}(s), \mathbf{M}(s)\}$. The force and moment read

$$\mathbf{R}(s) = R_x(s)\,\mathbf{e_1} + R_y(s)\,\mathbf{e_2} = N(s)\,\boldsymbol{\tau} + T(s)\,\mathbf{n}\,, \tag{10a}$$

$$\mathbf{M}(s) = M(s)\,\mathbf{e_3}\,. \tag{10b}$$

The quantity N is the axial (perpendicular to the cross-section) force along the beam axis, T is the shear force and M is the bending moment with respect to the $\mathbf{e_3}$ direction. The resultants in force and moment acting on the beam cross-section are functions of the strain measures defined in the above section. The elastic behavior of the beam is assumed to be linear with respect to the strain measures. Accordingly, the constitutive equations are stated as

$$N(s) = E\mathcal{A}\,\varepsilon(s)\,, \tag{11a}$$

$$M(s) = EI\kappa(s)\,, \tag{11b}$$

where E is the Young modulus, $\mathcal{A}$ the area of the cross-section (in the present case $\mathcal{A} = b\,h$) and I is the moment of inertia of the cross-section with respect to the $\mathbf{e_3}$ direction. In addition, $E\mathcal{A}$ and EI are the axial beam and bending stiffnesses, respectively.

3 Variational formulation for the buckling bistable beam

3.1 Principle of virtual work

To obtain the beam equations, we adopt the principle of virtual work. The principle for the present model of beam and configuration is stated as follows (in the static case)

$$\delta\mathcal{S} \ = \delta\mathcal{W}_i + \delta\mathcal{W}_e = 0\,. \tag{12}$$

The different contributions to the principle are $\mathcal{W}_i$ for the work of internal forces, $\mathcal{W}_e$ for the work of the applied actions.

The virtual work of internal forces of an elastic beam takes on the general form (the details of the algebraic manipulation can be found in (Camescasse *et al.* , 2013))

$$\delta\mathcal{W}_i = -\int_0^{L_0} \{\mathbf{R}(s) \cdot \delta\mathbf{q}'(s) + \mathbf{M}(s) \cdot \delta\mathbf{p}'(s) - (\mathbf{q}'(s) \times \mathbf{R}(s))\,\delta\mathbf{p}(s)\}\,ds \tag{13}$$

where "$\times$" denotes the vector product. We recall that the vector $\mathbf{q}(s)$ is the position vector of the material point $G(s)$ (see Eqn. (2)) and $\mathbf{p} = \theta\,\mathbf{e_3}$ is the vector rotation of the beam cross-section.

The bistable beam is subject to a lineic density of force applied into the beam staying in $(\mathbf{e_1}, \mathbf{e_2})$-plane. The virtual work of this density of force reads

$$\delta\mathcal{W}_e = \int_0^{L_0} \mathbf{F}(s) \cdot \delta\mathbf{q}(s)ds \tag{14}$$

where $\delta\mathbf{q}(s)$ is the virtual displacement of the material point $G(s)$ belonging to the deformed beam.

3.2 Dimensionless equations

For the sake of consistency and in order to highlight some key parameters, we introduce dimensionless variables and parameters, defined by

- *lengths* $\qquad\qquad (S, \mathbf{Q}, \Delta\ell) = (s, \mathbf{q}, \Delta L) / L_0\,,$ (15a)

- *Forces and moments* $\qquad (\mathsf{N}, \mathsf{T}, \mathsf{P}, \mathbf{M}) = (N/F_0, T/F_0, P/F_0, \mathbf{M}/M_0)\,,$ (15b)

- *Density of forces* $\qquad \mathsf{F} = \mathbf{F}L_0/F_0\,,$ (15c)

- *Energy* $\qquad\qquad \mathcal{E} = E_{tot}/E_0\,,$ (15d)

where the reference parameters have been defined as $F_0 = E\mathcal{A}k$, $M_0 = EI/L_0$ and $E_0 = F_0 L_0$. Moreover, the following key parameter has been introduced

$$k = \frac{I}{\mathcal{A}L_0^2} \tag{16}$$

which characterizes the ratio of the compression energy over the bending energy. The parameter $k \propto (h/L_0)^2$ where L_0/h is the slenderness ratio of the beam. Now, with the new dimensionless variables the position vector takes the form

$$\mathbf{Q}(S) = Q_X(S)\,\mathbf{e_1} + Q_Y(S)\,\mathbf{e_2} = Q_T(S)\,\boldsymbol{\tau} + Q_N(S)\,\mathbf{n} \tag{17}$$

which is the position vector of any material point of the beam at the curvilinear abscissa S written either in the fixed frame or in the local frame. The different coordinates in Eqn. (17) satisfy the dimensionless definitions introduced in Eqn. (15).

We now propose a new form for the variational equation Eqn. (12). However, the variational equation is written with the variables defined in the local frame. It reads as

$$\delta\mathcal{S}[\mathbf{Q}, \theta] = \int_0^1 \{(\mathsf{N}' - \theta'\mathsf{T})\,(\delta Q_T - Q_N\delta\theta) + (\theta'\mathsf{N} + \mathsf{T}' - \mathsf{F})\,(\delta Q_N + Q_T\delta\theta)\}dS$$
$$+ \int_0^1 \{\mathsf{M}' + (1 + \varepsilon)\,\mathsf{T}\}\delta\theta dS = 0\,. \tag{18}$$

It has been assumed here that $\mathsf{F} = \mathsf{F}\,\mathbf{n}$, that is, every element of force density is perpendicular to the deformed bistable beam. Obviously, in the algebraic manipulations leading to Eqn. (18), we accounted for the boundary conditions at the end of the beam. In particular, for clamped boundary conditions we have $\delta\theta = 0$ and $\delta\mathbf{Q} = \mathbf{0}$, because the displacement and the rotation of the beam at its ends are given.

3.3 Equations for the bistable buckled beam

The variational equation Eqn. (18) must be satisfied for any arbitrary variation $\delta\mathbf{Q}$ and $\delta\theta$ which meets the boundary conditions at $S = 0$ and $S = 1$ (clamped-clamped beam). We deduce the equations of the bistable beam as

$$\mathsf{N}' - \theta'\mathsf{T} = 0\,, \tag{19a}$$

$$\theta'\mathsf{N} + \mathsf{T}' - \mathsf{F} = 0\,, \tag{19b}$$

$$\mathsf{M}' + (1 + \varepsilon)\,\mathsf{T} = 0\,. \tag{19c}$$

Along with the above equations the associated boundary conditions read as

$$\mathbf{Q}(0) = \mathbf{0}, \qquad \mathbf{Q}(1) = X_B\,\mathbf{e_1}, \qquad \theta(0) = 0, \qquad \theta(1) = 0\,. \tag{20}$$

In the second boundary equation Eqn. (20), X_B denotes the abscissa of the right end of the beam due to the end-shortening of the clamp B. With the view of completing the above differential equations, it is convenient to write the geometrical equations Eqns. (9) in non-dimensional notation

$$Q'_T - \theta' Q_N = 1 + \varepsilon\,, \tag{21a}$$

$$Q'_N + \theta' Q_T = 0\,. \tag{21b}$$

A similar transformation holds for equations Eqns. (5). Their form using the non-dimensional notation introduced in Eqn. (15) can be obtained easily.

Now, we have almost all the ingredients to solve the problem of a bistable buckled beam subject to a density of lineic force. It is worth noting that each elementary lineic force is always perpendicular to the deformed beam while the beam is snapping.

At first sight, we have a set of nonlinear differential equations with given boundary conditions. This kind of problem is not trivial because first of all, there exist unstable equilibrium regions spanned while the beam switches from one stable state to the other one. In addition, the classical method cannot capture the configuration of the beam in the unstable region. The second difficulty is that at each step of the process method, the configuration of the lineic density force is modified because the density force is always normal to the deformed beam which is an unknown of the problem. Therefore, a more sophisticated algorithm to solve the problem becomes necessary.

4   Numerical analysis and results

4.1   Problem statement

This section is devoted to the numerical investigation of the nonlinear boundary value problem governing the snap-through of the bistable buckled beam. The equations to be solved were obtained in the previous Section. More precisely, they are the equations of the beam equilibrium Eqns. (19) and the geometric relationships Eqns. (21).

We recall that the axial strain and bending moment satisfy the constitutive equations Eqns (11) written in dimensionless form as

$$\varepsilon = k\,\mathsf{N}, \qquad\qquad \mathsf{M} = \theta'\,. \tag{22}$$

Note that at the ends A and B of the beam we have $\boldsymbol{\tau} = \mathbf{e_1}$ and $\mathbf{n} = \mathbf{e_2}$. In the set of equations Eqns. (19), Eqns. (21) have been included to compute the local displacement Q_N and Q_T as function of θ and N and boundary conditions concern those displacements. The set of equations that meets the boundary conditions (clamped-clamped beam) reads as

- At the A end ($S = 0$)

$$\theta(0) = 0, \tag{23a}$$

$$Q_T(0) = 0, \tag{23b}$$

$$Q_N(0) = 0. \tag{23c}$$

- At the B end ($S = 1$)

$$\theta(1) = 0, \tag{24a}$$

$$Q_T(1) = X_B, \tag{24b}$$
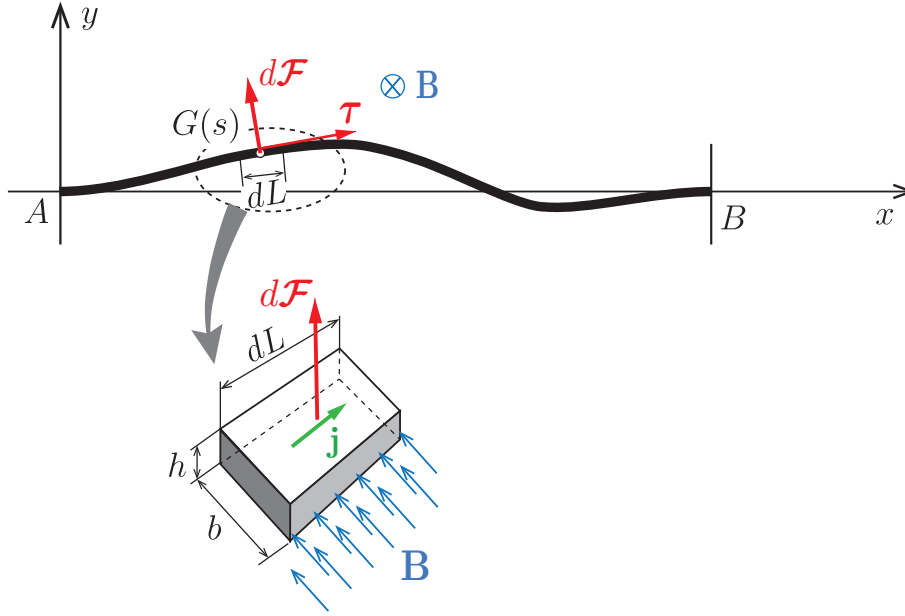
$$Q_N(1) = 0. \tag{24c}$$

Figure 3: Clamped-clamped buckled elastic beam: the Laplace force acting on the deformed beam and detail of an element of beam undergoing Laplace force produced by a volume density of moving electric charges placed in a magnetic induction.

Figure 3 shows the sketch of the clamped-clamped buckled beam for a given density of lineic force while switching. The detail of the lineic density produced by Laplace force is also shown, especially the induction field and the vector of electric current density par unit of area. In classical electrodynamics, the Laplace force acting on a small part of elementary volume dv of the beam is given by (Jackson , 1998)

$$d\boldsymbol{\mathcal{F}} = \mathbf{j} \times \mathbf{B}\, dv \tag{25}$$

where $\mathbf{j}$ is the density of electric current per volume unit such that $dv = \mathcal{A}d\ell$ ($\mathcal{A} = b\,h$ being the beam cross-section area). On introducing the electric current per unit of length $i\,\boldsymbol{\tau} = \mathcal{A}\mathbf{j}$ where $\boldsymbol{\tau}$ is the unit vector tangent to the deformed beam, the Laplace force acting on a piece of the beam of length $d\ell$ is then

$$d\boldsymbol{\mathcal{F}} = i\, d\ell\, \boldsymbol{\tau} \times \mathbf{B}\,. \tag{26}$$

The beam is placed between two magnets producing the magnetic induction $\mathbf{B}$ assumed to be uniform in the volume between the two magnets. For a given magnetic induction $\mathbf{B}$, the only free

parameter is the electric current. It will be the control parameter.

4.2 Algorithm for solving the switching bistable beam problem

To solve the set of nonlinear equations Eqns. (19) using an algorithm based on a Runge-Kutta method, we need the initial values for N, θ, M and T at $S = 0$. At first sight, the values $N(0) = N_A$, $M(0) = M_A$ and $T(0) = T_A$ which are the clamping efforts are not known. Accordingly, a numerical shooting algorithm must be used (see (Ascher *et al.* , 1987) for the implementation method). The input parameters of the method are given by boundary condition Eqns. (23) and we start with an initial guess for the set of parameters $\{N_A, T_A, M_A = \theta'_A\}$. The objective parameters are given by Eqns. (24). Moreover, we do not know the buckling force $P = N_A$ since only the end-shortening of the right end of the beam is given. The buckling force P is therefore obtained by solving the buckled beam problem with loading set to zero ($F = 0$).

The boundary value problem to be solved is not trivial since we are faced with unstable branches of solution while the beam is switching from one stable state to the other one. To avoid the divergence of the algorithm and discrepancy of the final results, we control the vertical displacement of the material point of the beam at the curvilinear abscissa S_C such that $Q_X(S_C) = (1 - \Delta\ell)/2$. The idea is to increment the mid-point by a very small amount at each value $Q_Y(S_C) = Y_C$ that corresponds to an unique deformed beam, while a same density of lineic actuating force can produce, *a priori*, different beam deformations.

A second numerical method is proposed to ascertain the first one, based on the finite element method. More precisely, we take the advantage of the FEniCS numerical libraries (Logg , 2012). The numerical code deals with the minimization of the total potential energy associated to the bistable beam and its actuating energy. The problem at hand is to find the equilibrium configurations, as with the first method. The difficulty is that for a given loading, different beam deformations can be obtained. We must have recourse to a more sophisticated algorithm using a so-called *deflated continuation method* by varying iteratively the loading parameter (Farrel , 2016) in order to capture the successive bifurcation points and the associated beam equilibria that can be either stable or unstable.

4.3 Results and comments

The forthcoming results have been obtained for a thin elastic beam made of amagnetic stainless steel A316L with a Young modulus of $E = 207$ GPa, length of 60 mm, width of 5 mm and thickness of 0.05 mm. The average magnetic induction between both magnets is about 0.3 Tesla. One of the first numerical results is the beam response under the density of lineic force produced by the Laplace force. Using the numerical method we compute the actuating force or, more conventently, the electric current, as function of the mid-point displacement of the beam. For a given end-shortening, the vertical displacement at the material point S_C of the beam is controlled step by step by varying the vertical position Y_C from the upper stable position to the lower one and *vice versa*. The numerical algorithm enables us to compute the corresponding actuating lineic density of follower force. Using the Laplace force equation Eqn. (26) we deduce the corresponding electric current in the beam.

The electric current as function of the mid-point beam displacement $y_m = Y_C L_0$ is shown in Fig.4. A classical N-shaped curve is obtained for three different end-shortenings: (i) weak (small end-shortening 0.3% of the beam length), (ii) intermediate (end-shortening of 1%) and (iii) rather
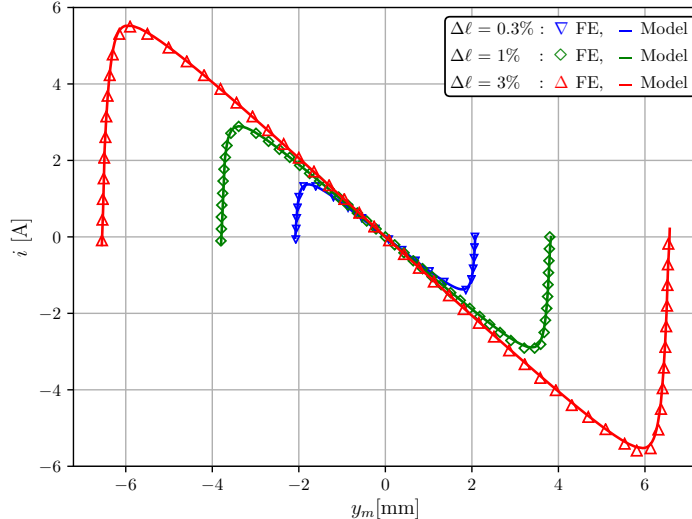
Figure 4: Bistable response: electric current as function of the beam mid-point displacement for three different values of the beam end-shortening (in solid line: the elastica model, small triangles and diamonds: FE results).

large (large end-shortening of the order of 3% or great buckling deflection). At first sight, the curves are quite similar in shape. The present results can be compared to those obtained with a punctual force actuation (Camescasse *et al.* , 2013). The part of the force-displacement diagram which is almost a line corresponds to the unstable region. Note that all the curves pass through zero ($y_m = 0$, $i = 0$), and are symmetric with respect to the origin. Moreover, all the curves display a negative slope between extrema, which means that the bistable system possesses a negative stiffness on this part of the branch, which corresponds to instability. An important comment from the present results is that both numerical methods give quite similar results, which confirms the robustness of the modeling of the bistable buckled beam based on elastica theory. The results are applied not only for weak buckling deflection but also for rather large deflection in comparison to the beam slenderness. The concept of Laplace force is not so easy to handle. A question which could be raised is what would be the bistable response if the Laplace force is replaced by vertically fixed force? This point is discussed in Appendix A.

The second result extracted from the numerical simulations is the compressive force P applied at the right end of the beam in order to maintain a given end-shortening as function of the displacement computed at the beam mid-point. The results for three different values of the end-shortening are reported on Fig.5.

We observe that, for each curve, the compressive force for null loading corresponds to the buckling critical force depending on the chosen end-shortening. As soon as the electric current is switched on and it begins to increase, the compressive force increases rapidly as well until it reaches a plateau. As in the previous results the comparison of both numerical approaches gives very close results, which confirms, once more, the reliability of the present modeling based on elastica beam theory. Instructive results can be obtained by computing the total potential energy. We recall that the numerical using FE method is based on the minimization of the total potential energy of the system. The latter reads as

$$\mathcal{E} = \int_0^1 \left(\frac{1}{2} \mathsf{M} \kappa + \frac{1}{2k} \mathsf{N} \varepsilon \right) dS \,. \tag{27}$$

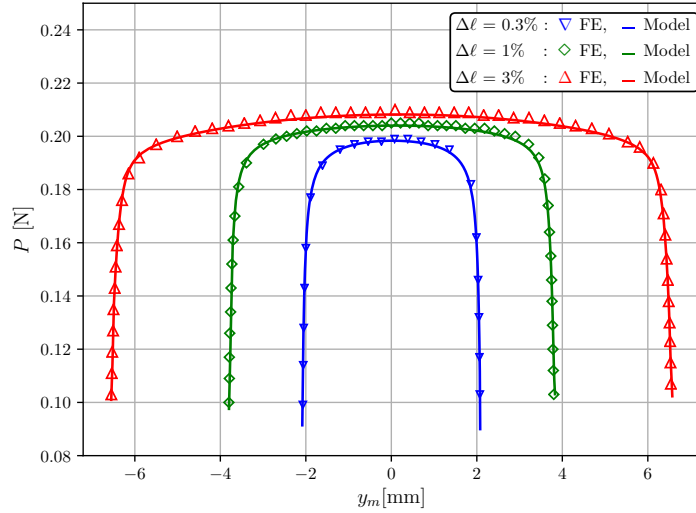The first term on the right hand side in Eqn. (27) represents the density of bending energy and

Figure 5: Bistable response: compressive force or buckling loading as function of the beam mid-point displacement for three different values of the beam end-shortening (in solid line: the elastica model, small triangles and diamonds: FE results).

the second term is the energy density of compression. The potential energy is computed using the results from the numerical simulations of the model equations (see Eqns. (19)) for each configuration of the deformed beam while the beam is snapping. Figure 6 shows the variations of the total potential energy as function of the beam deflection at the beam mid-point from the upper stable position to lower one and *vice versa*. The FE results have been superposed to the results of the first method in Fig.6. It worth noticing that the potential energy possesses two minima corresponding to the stable positions of the bistable beam. The relative error between both numerical results is less than 0.4%.
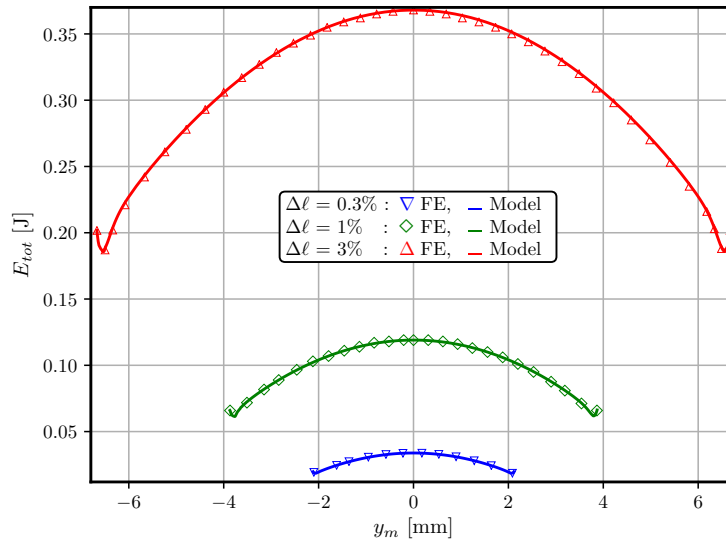

Figure 6: Bistable response: Total potential energy as function of the beam mid-point displacement for three different values of the beam end-shortening (in solid line: the elastica model, small triangle and diamonds: FE results).

One of the advantages of the elastica model and the path-following technique used to solve the nonlinear boundary value problem is that we are able to capture with enough accuracy the beam

deformation when passing through the zone of instability of the bistable system. However, for rather small end-shortening, the beam cross-section rotation and displacements have small amplitudes. Therefore, the equations for the bistable beam can be linearized. More precisely, the set of equations Eqns. (19 and 21) are linearized with zero actuating loading ($\mathsf{F} = 0$) around the critical buckling force P_c for $\mathsf{P} > \mathsf{P}_c$. Trivial algebraic manipulations lead to the following equation for the beam deflection

$$Q_Y^{(4)} + \mathsf{P}\left(1 - k\mathsf{P}\right)Q_Y'' = 0\,. \tag{28}$$

Here we recover the classical Euler equation for a buckling beam; however, in Eqn. (28) the buckling force P is altered by the factor $(1 - k\mathsf{P})$ accounting for the compressibility of the beam in the pre-buckling regime. We point out that the deflection of the beam Q_Y has been chosen instead of the rotation θ because the deflection must satisfy four boundary conditions at the ends of the beam, which not the case for the rotation. Eqn. (28) possesses two kinds of solution (symmetric and asymmetric modes) satisfying the boundary conditions for clamped-clamped beam, namely $Q_Y\left(0\right) = 0$, $Q_Y'\left(0\right) = 0$, $Q_Y\left(1\right) = 0$, $Q_Y'\left(1\right) = 0$. Appendix B provides the buckling mode solutions to Eqn. (28) along with the associated boundary conditions. Going back to the solution deduced from the numerical simulations of the boundary value problem, we can write the solution as an expansion of the buckling modes

$$Q_Y\left(S\right) = \sum_{j=1}^{J} A_j Y_j\left(S\right) \tag{29}$$

where $Y_j\left(S\right)$ are the buckling modes (see Appendix B for their exact forms). The factors A_j correspond to the contribution of the modes. The first derivatives (and also the second derivatives) form an orthogonal vectorial base. Therefore, by multiplying the derivative of the expansion Eqn. (29) with respect to S by the j's buckling mode, we arrive at

$$A_j = \left\langle Q_Y'\left(S\right), Y_j'\left(S\right)\right\rangle \tag{30}$$

where $\left\langle \cdot, \cdot \right\rangle$ is the scalar product in the functional space $\mathsf{L}^2[0,1]$.

The result of the computation is shown in Fig.7 for the first five modes. We observe that the first mode is predominant in the vicinity of the stable positions, and that its influence decreases rapidly when the bistable is switching as the second buckling mode takes over from the first one. When the bistable passes through a zero deflection at the mid-point of the beam, the second mode prevails, and the bistable is in the region of instability. Fig.7 gives interesting information about the buckling mode contribution, especially the third mode, which is an even mode. It plays a significant role in the switching process since 30 per cent are involved in the snapping scenario. The other modes, the fourth and fifth are not really significant, as their contributions are less then 4%. This result demonstrates that if we want to use a reduced model, the first three buckling modes should be enough to describe the beam switching in the framework of small end-shortenings. Fig. 8 summarizes the beam deflection at the different step of the snapping process.

On using the path-following procedure with the control parameter defined by vertical coordinate of the crossing point of the beam with the vertical line fixed at the mid-point between both clamps, we are able to capture, step by step, the beam deformation. More precisely, when the bistable is switching, the crossing point moves along the vertically fixed line. To each crossing point corresponds a unique beam deformation. Accordingly, the switching scenario can be seen as follows : (a) when the actuating force is zero the bistable beam deformation corresponds to the first buckling mode; (b) when the electric current increases, the beam mid-point increases as well; however, for a strong enough lineic force, the beam starts snapping, accordingly the beam
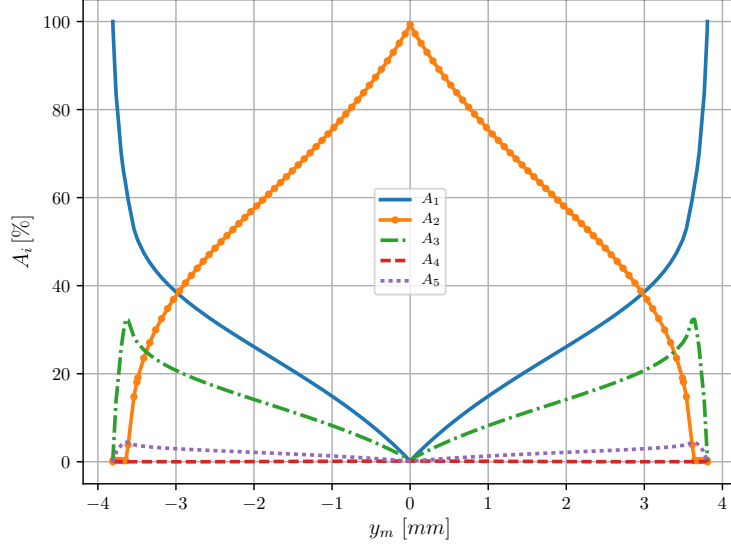
14

Figure 7: Contributions of the first five buckling modes in the snap-through process (in percent) for an end-shortening of 1% of the total length.
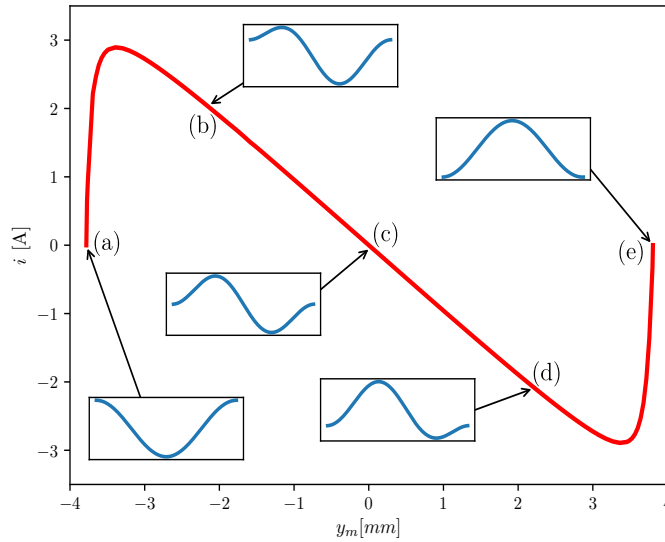

Figure 8: Switching scenario of the bistable beam, (a) beam at the lower stable position, (b) region of instability, combination of buckling modes, (c) second buckling mode, (d) beam profile symmetrically inverted with respect to that at (b), (e) beam at the upper stable position.

profile is mainly a combination of the first three buckling modes with the mode contribution given in Fig.7; (c) the bistable beam is passing through the domain of instability, the electric current must be decreased, the beam mid-point passes through zero, the second buckling mode is therefore predominant; (d) the beam mid-point continues to increase and we recover the profile of the beam at point (b), but symmetrically inverted and finally; the beam ends its running at the upper stable position (e) and we recover the first buckling mode, but upside down.

5   Experimental validations

This section reports an effort to bridge the modeling approach presented in the above sections with experimental observations. The emphasis is placed on the validation of the bistable response in

electric current (lineic density of force) as function of the mid-point vertical displacement of the beam subject to electromagnetic Laplace force. Comparisons of the proposed experimental results to those derived from the bistable beam based on elastica theory will be discussed. A thin elastic beam having the same dimensions and material properties as used in the analytical and numerical studies was fabricated for the experiment (see Section 4.3).

5.1 Description of the experimental set up and process of measures

The thin elastic beam is manufactured from a sheet of amagnetic stainless steel A316L using electro-eroding process. Several test beams have been cut with an accuracy of less than $1/100$ mm. Particular attention is paid to obtaining a high quality planar beam with a minimum of residual stress. The beam is thus subject to metallurgical process consisting in heating at 500^0C in an oven for few hours and maintained absolutely planar and then in cooling gradually to the ambiant temperature.

The thin beam is placed between two clamps which maintain the beam ends very tightly. Fig.9 shows the photos of the complete experimental set-up. The test set-up is equipped with a micro-metric translator at one of the beam ends. The translator allows us to control the displacement of the beam ends (the right end) while the other is fixed. Using travel translator stage we are able to monitor the end-shortening of the beam with $10\,\mu$m adjustment (see Fig.9). Moreover, a digital micrometer with an accuracy of $1\,\mu$m is used in order to control the displacement of the platform of the moving clamp.
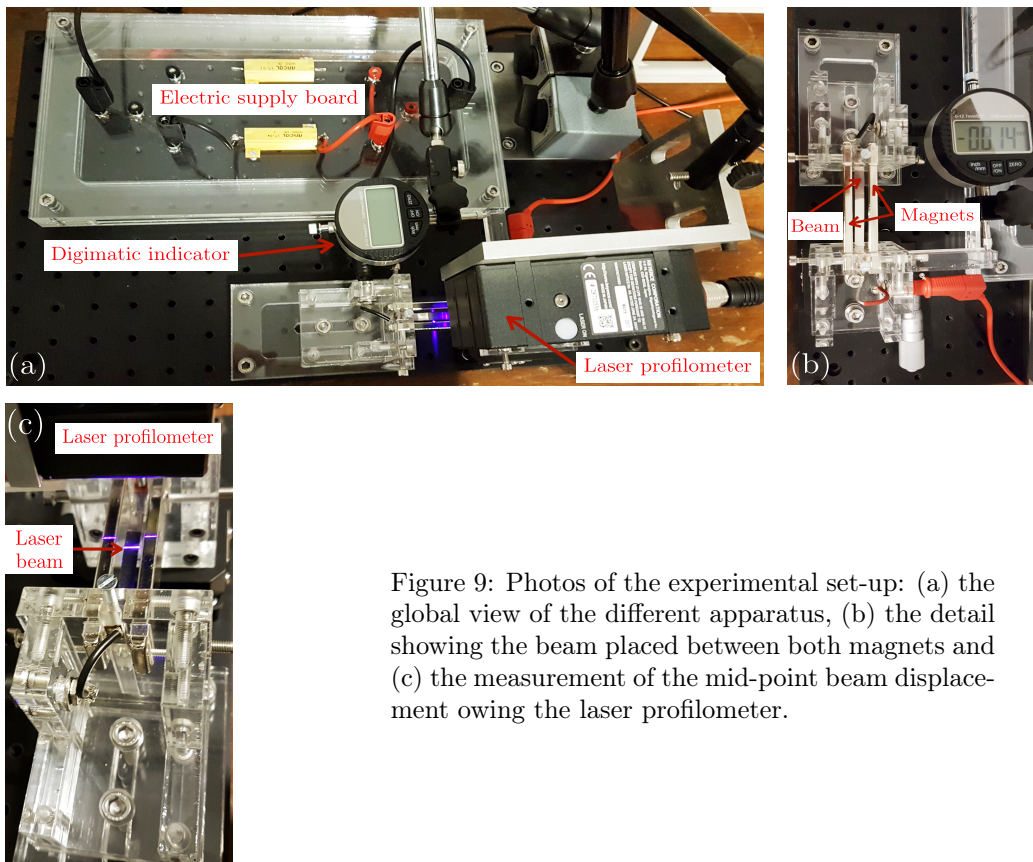

Figure 9: Photos of the experimental set-up: (a) the global view of the different apparatus, (b) the detail showing the beam placed between both magnets and (c) the measurement of the mid-point beam displacement owing the laser profilometer.

The beam is placed between two magnets of neodyme type (NdFeB alloy) length of 80 mm, height of 17 mm and thickness of 5 mm. The gap between both magnets is 8 mm. The magnetic induction has been measured with the help of Gaussmeter equipped with a Hall effect probe. The magnetic induction is about 0.3 Tesla. In addition an electric current supply provides a given stable electric

current through the beam, in series with a power resistor in order to dissipate the electric power into heat.

A schematic diagram of the experiment set-up is shown in Fig.10. The measurement process begins by applying a given end-shortening using the travel translator stage. The end-shortening for the tests is controlled thanks to a digital comparator measuring the exact displacement of the moving clamp. For a given end-shortening the electric current is monitored by a computer and it is increased step by step from zero until the electric current produces a strong enough lineic density of force to trigger the beam snap-through. The bistable beam reaches the lower stable position. A Keyence ultra-high speed laser profilometer model LJ-V7060 (blue semi-conductor laser of wavelengh 505 nm, output power of 10 mW, measurement range in Z-axis (heigh) : ± 8 mm, in X-axis (width) : 13.5 mm) enable to measure the variation of the vertical displacement at the mid-point beam. Both evolutions of the electric current travelling the beam and the mid-point beam displacement are correlated and sent to a computer. The process is stopped immediately after the snap-through has been detected. The profiler signal is sent out to the computer in order to analyze the digital signal and convert it into an analogic displacement of the beam center. The process is repeated for switching from bottom stable position of the beam to the top one.
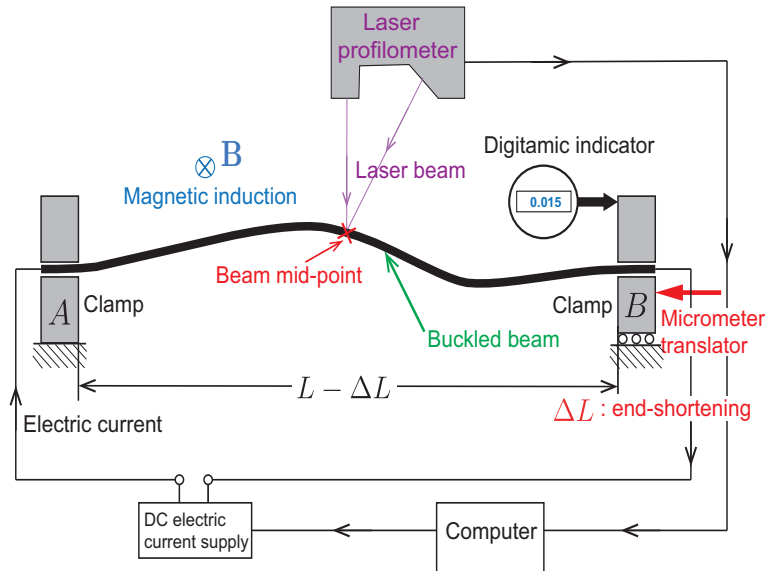

Figure 10: Diagram of the experimental set-up showing the principal experimental apparatus.

5.2 Experimental measurement and discussion of the results

Bifurcation diagram. One of the first experimental results concerns the bifurcation diagram, namely, the beam deflection at its center as function of the end-shortening when actuation is set to zero. On using the travel translator we impose the desired end-shortening at the right end of the beam. The end-shortening is read directly on the digital comparator. The beam deflection at its center is measured thanks to the laser profilometer and the value is transmitted to the computer. Accordingly, by varying the axial translation we obtain first, the value of the end-shortening and then, the corresponding deflection of the beam. Figure 11 shows the bifurcation diagram. The experimental data are depicted by small red points and they are superimposed to the result deduced from the numerical simulations (the curve in solid line). We notice a strong fit between the model and experimental data. Obviously, because of the high slenderness ratio of the beam $\frac{L}{h} = 12000$, the pre-buckling zone is so tiny that it is not observable.
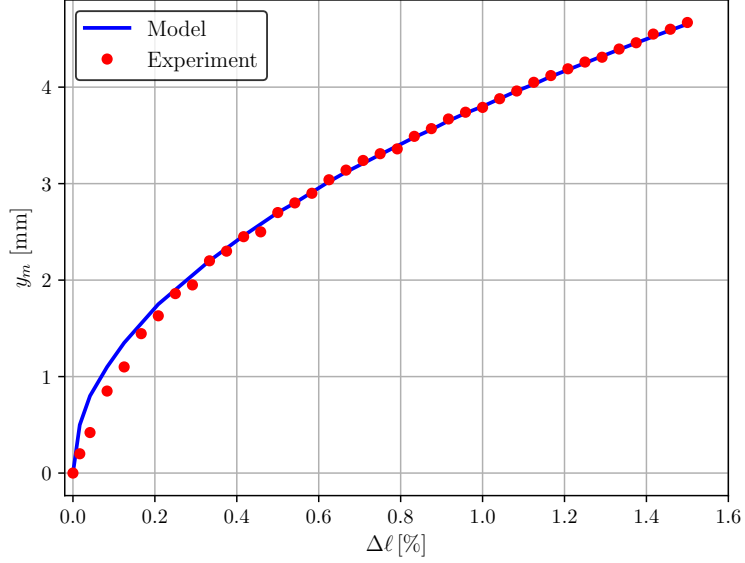
Figure 11: Diagram of bifurcation: beam center deflection as function of the end-shortening. Experimental results: red spot, model: blue solid line

Bistable response to applied Laplace actuation. The experimental results are depicted in Fig.12. The experimental data are superimposed to the analytical results; the continuous lines correspond to the stable phase and the unstable region is plotted in dashed line. This part of the bistable response region cannot be experimentally characterized. Referring to the results given by the bifurcation diagram (Fig.11), we choose different interesting values of the end-shortening and we identify the corresponding beam center deflections. The experimental data are marked by small symbols (small circles, triangles or squares). First of all, we observe that experimental points are very close to the analytical results, yielding a strong validation of the present model. This is true for different end-shortening values. The error between the results coming from the numerical simulations of the model equations and the experimental data stays within a segment of less than 2%.
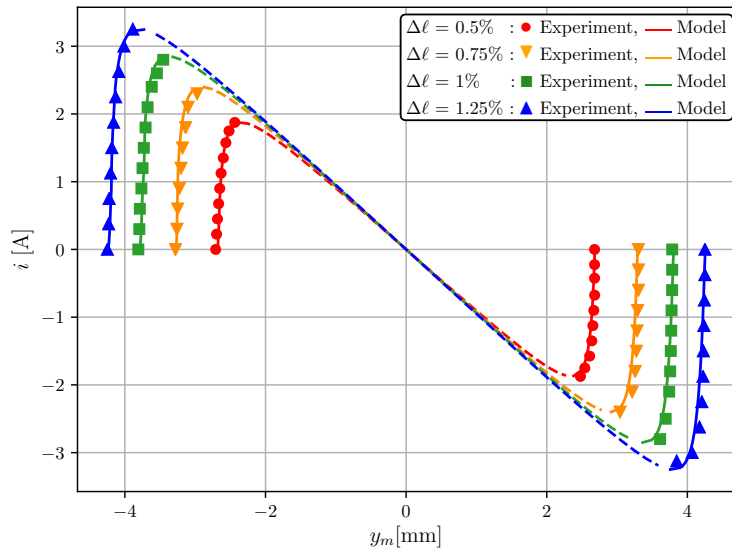

Figure 12: Bistable response: experimental results superposed onto the numerical simulations of the bistable beam model.

6   Discussion and concluding remarks

The main objective is to develop and analyze a model for bistable buckled beam based on an elastica approach of beam, including extensibility. On using the complete model that is, by considering rotations and displacements of large amplitudes, we examine in detail the switching process of the bistable beam. The beam actuation is produced by a lineic density of uniform force. This means that the force configuration follows the beam deformation variation while the bistable transits from one stable position to the other one. As a matter of fact such an actuating force can be produced by an electromagnetic Laplace force. The latter is due to the electric current travelling in the beam placed in a magnetic induction.

The most pertinent results describing the switching process of the bistable buckled beam are obtained first with the use of semi-analytical solution by solving the nonlinear boundary value problem. At last, experimental validation of the bistable beam actuated by an electromagnetic Laplace force is proposed and confirms with a high quality of accuracy the present model, which demonstrates that this apparently simple bistable system actuated by a contactless process is rich enough to provide particularly interesting comments :

- The bistable modeling in the elastica theory framework allows us to write down the governing beam equation for transformation of large amplitudes. The equations of the nonlinear boundary value problem are deduced from a variational formulation. Moreover, the equations of the bistable beam are written in the local referential frame attached to the actual configuration of the beam (deformed beam).

- Important results concern the response of the bistable beam to the Laplace force. The responses have been computed for several end-shortening values and they describe the evolution of the electric current (through the computed applied lineic force) as function of the vertical displacement of the beam mid-point. The response exhibits an N-shaped curve. The numerical algorithm is efficient enough, which allows us to capture the beam configurations at each step of the vertical increment, even for unstable branches. A second numerical investigation based on the FE method and path following procedure is also reported. The results of the second numerical method confirms perfectly the first numerical results, especially the robustness of the beam modeling based on elastica beam theory.
  Among the results which can be extracted from both numerical investigations, we have examined (i) the bistable response, the electric current as function of the displacement of the beam mid-point, (ii) the buckling loading applied to one of the beam ends to maintain the given end-shortening, (iii) the total potential energy exhibiting minima at the each stable position of the buckled beam (upward and downward) and (iv) the analysis of buckling modes and their precise contribution to the snapping process.

- Finally, a section is devoted to experimental tests which have ascertained the validity of the model. The comparisons between the experimental tests and numerical results are quite good, with very small discrepancies. In short, a good correspondance is observed between the bistable response modeling prediction and experimental results, which establishes a reliable validation of the present model.

All the results presented in this study are good reasons to undertake complementary and forthcoming works, on the nonlinear dynamics of the bistable beam in the post-buckling regime when applying time-dependent electric current through the beam. Experimental investigations will have to be considered to confirm the model predictions. The model along with the obtained results

opens new views to design innovative devices in the area of micro-robotics, medical engineering, etc.

Appendix A Comparison with bistable switching by means of a lineic density of vertically fixed force.

A question that we might ask ourselves is what would the bistable beam response be if the Laplace force was replaced by a lineic density of force with fixed vertical direction. Would there be a noticeable difference? To understand the problem better, we performed a numerical simulation of the bistable response subject to a lineic fixed force. The result is illustrated in Fig.13. The curves are superposed for the same end-shortening of 3 % and for the same order of lineic density of force. A difference is clearly observed, as the maximum of lineic density of follower force actuation is little bit greater than that of the vertically fixed force. In addition, the relative difference between maxima have been computed and presented in Fig.14. The relative difference is defined by
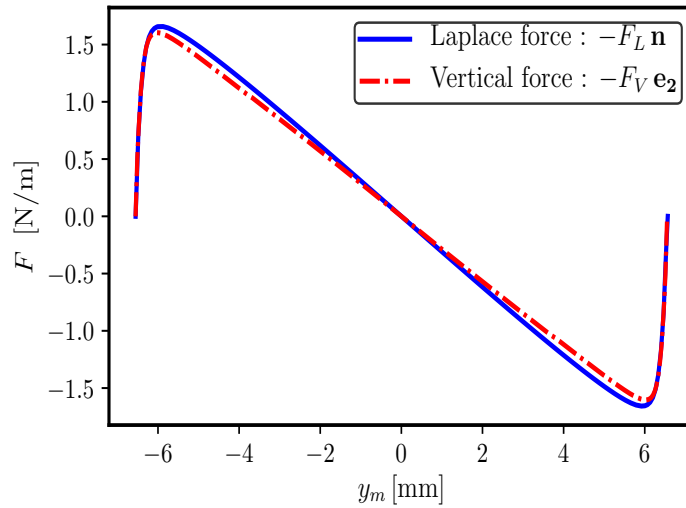

Figure 13: Lineic density of force as function of the beam mid-point displacement. Comparison between bistable actuations by means of lineic density of Laplace force and vertically fixed force. Laplace force (in solid line) and vertically fixed force (dashed line).
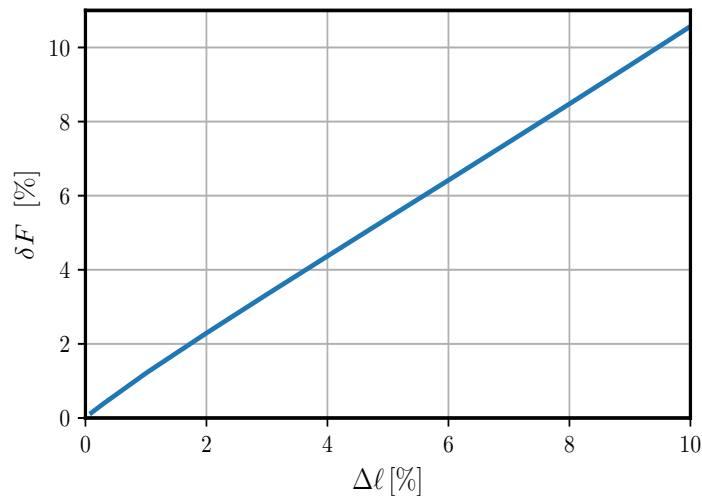

Figure 14: Relative difference between bistable actuations by means of lineic density of Laplace force and vertically fixed force.

$\delta F = \left(F_L^{(max)} - F_V^{(max)} \right) / F_L^{(max)}$ where F_V is for the vertical force and F_L referred to the Laplace force. We notice that δF increases with the end-shortening. For instance, an end-shortening of the order of 5% gives rise to a relative difference between both kinds of actuation of about 5.4%. Accordingly, we cannot reasonably use the lineic density of vertically fixed force as an approximation of the Laplace force.

Appendix B   Buckling modes for a clamped-clamped beam

The buckling modes are obtained by solving Eqn. (28), accounting for the boundary conditions for a clamped-clamped beam. The solution splits into two kinds of modes.
(i) The symmetric buckling modes read as

$$Y_j(S) = A_j(1 - \cos(\alpha_j S)) \tag{B.1}$$

with

$$\alpha_j = 2j\pi \tag{B.2}$$

Moreover, we have set $\alpha^2 = \mathsf{P}(1 - k\mathsf{P})$ in Eqn. (B.1).
(ii) The antisymmetric modes are given by

$$Y_j(S) = A_j\left\{1 - \cos(\alpha_j S) \ - \frac{2}{\alpha_j}(\alpha_j S - \sin(\alpha_j S))\right\} \tag{B.3}$$

where now the values of α_j are the solutions to the implicit equation

$$\tan\left(\frac{\alpha_j}{2}\right) = \left(\frac{\alpha_j}{2}\right) \tag{B.4}$$

In Eqns (B.1) and (B.3) A_j is an amplitude that we have at hand to be adjusted in order that the mode is normalized.

Acknowledgements

References

Aimmanee S., Tichakorn K., Piezoelectrically induced snap-through buckling in a buckled beam bonded with a segmented actuator. J. Int. Mat. Sys. and Struc. DOI: 10.1177/1045389X17754270 (2018).

Ascher U.M., Mattheij R.M.M., Russell R.D., Numerical solution of boundary value problem for ordinary differential equations. SIAM, Philadelphia, 1987.

Bazant Z .P., Cedolin L., Stability of structures. Oxford University Press, New York, 1991.

Bigoni D., Nonlinear solid mechanics : bifurcation theory and material instability. Cambridge University Press, Cambridge, 2012.

Buchaillot L., Millet O., Quevy E., Collard D., Post-buckling dynamic behavior of self-assembled 3D microstructures. Microsyst. Technol. 14, 69 -78 (2008).

Camescasse B., Fernandes A., Pouget J., Bistable buckled beam: Elastica modeling and analysis of static actuation. Int. J. Solids and Structures 50, 2881 - 2893 (2013).

Camescasse B., Fernandes A., Pouget J., Bistable buckled beam and force actuation : Experimental validations. Int. J. Solids and Structures 51, 1750 - 1757 (2014).

Cazottes P., Fernandes A., Pouget J., Hafez M., Bistable buckled beam : modeling and actuating force and experimental validations. ASME J. Mech. Des. 131, 1001001 - 1001011 (2009).

Cazottes P., Fernandes A., Pouget J., Hafez M., Design of actuation for bistable structures using smart materials. CIMTEC 2008, 3rd International Conference on Smart Materials, Structures and Systems, 8-13 June, 2008, Acireale, Sicily, Italy.

Chandra Y., Stanciulescu I., Virgin L.N., Eason T.G., Spottswood S.M., A numerical investigation of snap-through in a shallow arch-like model. J. Sound and Vibration 332, 2532 - 2548 (2013).

Chen J.-S., Hung S.-Y., Snapping of an elastica under various loading mechanism. Eur. J. Mech. A/Solids 30, 525 - 531 (2011).

Cleary J., SU H.-J., Modeling and experimental validation of actuating a bistable buckled beam via moment input. ASME J. of Applied Mech. 82, 051005-1 - 051005-7 (2015).

Das K., Batra R.C., Pull-in and snap-through instabilities in transient deformations of microelectromechanical systems. J. Micromech. Microeng. 19, 035008 (2009).

Dym C.L., Stability theory and its applications to structural mechanics. Dover Publications, New York, 2002.

Farrel P.E., Beentjes C.H., Birkisson Á. ,The computation of disconnected bifurcation diagrams. arXiv preprint arXix : 1603.00809.(2016).

Fernandes A., Maurini C., Vidoli S., Multiparameter actuations for shape control of biatable composite plates. Int. J. Solids Struct. 47, 1449 - 1458 (2010).

Griffiths, D.J., Introduction to electrodynamics (3rd ed.). Prentice-Hall, Upper Saddle River, [NJ.], (1999).

Herrera-May A.L., Aguila-Cortés L.A., Garcia-Ramirez P.J., Manjarrez E., Resonant magnetic field sensors based on MEMS technology. Sensors 9, 7785 - 7813 (2009).

Jackson, J.D., Classical electrodynamics (3rd ed.). John Wiley and Sons, New York (1998).

Krylov S., Dick N., Dynamic stability of electrostatically actuated initially curved shallow microbeams. Continuum Mech. Thermodyn. 22, 445-468 (2010).

Krylov S., Ilic B., Lulinsky S., Bistability of curved microbeams actuated by fringing electrostatic fields. Nonlinear Dynamics 66, 403-426 (2011).

Logg A., Marchal K.-A., Wells G., Automated solution of differential equations by the finite element method : The FEniCS book. Springer-Verlag New York Inc (2012).

Maugin G.A., Continuum mechanics of electromagnetic solids. North-Holland, Series Applied Mathematics and Mechanics, vol. 33 (Amsterdam, 1988).

Maurini C., Pouget J., Vidoli S., Distributed piezoelectric actuation of a bistable buckled beam. Eur. J; Mech. A/Solids 26, 837 - 853 (2007).

Medina L., Gilat R., Krylov S., Bistability criterion for electrostatically actuated initially curved micro plate. Int. J. Engng Science 130, 75 - 92 (2018).

Nayfeh H., Enam S.A., Exact solution and stability of post-buckling configurations of beams. Nonlinear Dynamics 54, 395-408 (2008).

Pane I.Z., Asano T., Investigation on bistability and fabrication of bistable prestressed curved beam. Japanese Journal of Applied Physics 47, 529 - 5296 (2008).

Park S., Hah D., Pre-shaped buckled-beam actuators : theory and experiments. Sens. Actuators A 148, 186 - 192 (2008).

Patricio P., Adda-Badim M., Ben Amar M., An elastica problem : instability of an elastic arch. Phys. D 124, 285 - 295 (1998).

Pinto O.C., Gonçalves P.B., Active non-linear control of buckling and vibrations of a flexible buckled beam. Chaos Solitons & Fractals. 14, 227-239 (2002).

Pippard A.B., The elastic arch and its modes of instability. Eur. J. Phys. 11, 359-365 (1990).

Schultz M.R., Hyer M.W., Williams R.B., Wilkie W.K., Inman D.J., Snap-through of ansymmetric laminates using piezocomposite actuators. Compos. Sci. Technol. 66, 2442 - 2448 (2006).

Seffen K.A., Vidoli S., Eversion of bistable shells under magnetic actuation: a model of nonlinear shapes. Smart Mater. Struct. 25, 065010 (2016).

Thomson J.M.T., Hunt G.W., A general theory of elastic stability. New York, N.Y. Wiley, 1973.

Timoshenko S.P., Gere J.M., Theory of elastic stability, 2nd Ed., McGraw-Hill.

Vidoli S., Maurini C., Tristability of thin orthotropic shells with uniform initial curvature. Proc. Roy. Soc. A/Math. Phys. and Engng. Sciences 464, 2949 - 2966 (2008).

Vangbo M., An analytical analysis of a compressed bistable buckled beam. Sensors and Actuators A69, 212-216 (1998).

Williams M.D., Van Keulen F., Sheplak M., Modeling of initially curved beam structures for design of multistable MEMS. ASME J. Applied Mech. 79, 011006-1 - 011006-11 (2012).